Data in Brief 16 (2018) 489–500

Contents lists available at ScienceDirect

Data in Brief

journal homepage: www.elsevier.com/locate/dib

Data Article

Dataset on the activation of Müller cells through macrophages upon hypoxia in the retina

Christina Nürnberg [a,*], Norbert Kociok [a], Claudia Brockmann [a], Timo Lischke [b], Sergio Crespo-Garcia [a], Nadine Reichhart [a], Susanne Wolf [c], Ria Baumgrass [b], Sabine A. Eming [d], Sandra Beer-Hammer [e], Antonia M. Joussen [a]

[a] Department of Ophthalmology, Charité – Universitätsmedizin Berlin, corporate member of Freie Universität Berlin, Humboldt-Universität zu Berlin, and Berlin Institute of Health, Berlin, Germany
[b] German Rheumatism Research Center Berlin, a Leibniz Institute, Berlin, Germany
[c] Department of Cellular Neuroscience, Max Delbrück Center in the Helmholtz Society, Berlin, Germany
[d] Department of Dermatology, University of Cologne, Germany
[e] Department of Pharmacology and Experimental Therapy and Interfaculty Center of Pharmacogenomics and Drug Research, University of Tübingen, Germany

ARTICLE INFO

Article history:
Received 14 October 2017
Received in revised form
15 November 2017
Accepted 16 November 2017
Available online 22 November 2017

ABSTRACT

The dataset presented in this article complements the article entitled "Myeloid cells contribute indirectly to VEGF expression upon hypoxia via activation of Müller cells" (C. Nürnberg, N. Kociok, C. Brockmann, T. Lischke, S. Crespo-Garcia, N. Reichhart, S. Wolf, R. Baumgrass, S.A. Eming, S. Beer-Hammer, and A.M. Joussen). This complementary dataset provides further insight into the experimental validation of the $VEGF^{fl/fl}$ LysMCre (here named $VEGF^{mcko}$) knockout model used in the main article through genomic and quantitative Real-Time PCR in various murine tissues as well as additional flow cytometry data and immunohistochemical stainings. By providing these data, we aim to enable researcher to reproduce and critically analyze our data.

DOI of original article: https://doi.org/10.1016/j.exer.2017.10.011
* Corresponding author.
E-mail address: Christina.Nuernberg@med.uni-heidelberg.de (C. Nürnberg).

https://doi.org/10.1016/j.dib.2017.11.062

Specifications Table

Subject area	Biology
More specific subject area	Medicine - Ophthalmology.
Type of data	Table, text file, graph, figure
How data was acquired	PCR processor (LightCycler 480, Roche, Basel Switzerland), FACS (LSRFortessa flow cytometer (BD Biosciences, Franklin Lakes, NJ, USA)), data analyzed with FlowJo software (version 9.8.1; Treestar, Ashland, OR, USA), Microscope (Axio Imager.M2 microscope (Zeiss, Jena, Germany)
Data format	Analyzed
Experimental factors	VEGF-A$^{fl/fl}$ LysMCre$^{tg/+}$ (here named VEGF^{mcko}) and C57Bl/6J were used as experimental animals. VEGF-A$^{fl/fl}$ LysMCre$^{+/+}$ (here named controls) were used as controls
Experimental features	qPCR: RNA-isolation was conducted with the NucleoSpin RNA Mini Kit (Machery Nagel, Düren, Germany) For reverse transcription of cDNA, the "High-Capacity cDNA Reverse Transcription Kit" (Applied Biosystems, Darmstadt, Germany) was used. FACS: Spleen, bone marrow and retina samples were mashed through cell strainer (70 µm for spleen and bone marrow and 40 µm for the retina). Afterwards, the cells were re-suspended in PBS, centrifuged and used for FACS analysis.
Data source location	Berlin, Germany
Data accessibility	Data are with this article
Related research article	Christina Nürnberg, Norbert Kociok, Claudia Brockmann, Timo Lischke, Sergio Crespo-Garcia, Nadine Reichhart, Susanne Wolf, Ria Baumgrass, Sabine A. Eming, Sandra Beer-Hammer, and Antonia M. Joussen. Myeloid cells contribute indirectly to VEGF expression upon hypoxia via activation of other cell types Müller cells. Exp. Eye Res. 2017.

Value of the Data

These data give an overview of the relative Cre mRNA expression in the retina as well as the genomic recombination efficiency in brain and bone marrow and the Cre and VEGF-A mRNA expression in brain, bone marrow and lung as part of the validation of the VEGF$^{fl/fl}$ LysMCre (here named VEGF^{mcko}) knockout mouse model. These data are important for the use of the same knockout mouse in other studies.

Flow cytometric data providing an overview of T memory cells, natural killer (NK) cells, and natural killer-T (NKT) cells as percentage of CD45 positive cells in the retina of knockout and control retinas under normoxic and hypoxic conditions are presented.

The presented pathological retinal features in the model of oxygen-induced retinopathy in clodronate-liposome treated mice is of interest for similar studies.

1. Data

Seven-day-old pups and the nursing dam were exposed to a 75% oxygen containing environment for five days before replacement in normal housing conditions causing a neovascular stimulus via relative hypoxia until further analysis on postnatal days 14 and 17. The oxygen box was opened daily for a very short period to check on pups and mother.

2. Experimental design, materials, and methods

The experimental procedures are described in the related research article: Nürnberg et al. [1] (Table 1). A more detailed description of some of the methods used in this article as followed Figs. 1-8:

3. Material and methods

3.1. Mouse model of oxygen induced retinopathy

Oxygen Induced Retinopathy (OIR) was induced as described in the main text with few modifications (Fig. 1). The nursing dam as well as the offspring was kept under normal housing conditions from day P0 to P7. On day P7 the animals were exposed to a 75% oxygen containing environment for five days using a special oxygen chamber (Model THF3384, EHRET Labor- u. Pharmatechnik GmbH, Emmendingen, Germany). In contrast to the original protocol [2], the oxygen chamber was opened once daily for a few minutes to check on dam and pups. On P12 the mice were transferred back into normal housing conditions until P14 or P17 for analysis. A surrogate dam was provided if the nursing dam passed away – a very rare occurrence though. Room air controls were kept under normal housing conditions at all times.

Table 1
Antibodies used.

Antibody	Concentration	Source	Catalogue Number
Rabbit-anti GFAP	1:250	DAKO	Z0334
Mouse anti-Vimentin	1:50	Santa-Cruz	sc-32322
Goat anti-rabbit IgG Cy3	1:200	Dianova	111–165-144
Rabbit anti-mouse IgG Alexa488	1:200	Invitrogen	A11059
Rabbit anti-VEGF-A	1:100	Abcam	ab46154
Donkey anti-rabbit AlexaFluor488	1:10.000	Invitrogen	A-21206
Rabbit anti-CD11b	1:100	Novus Biologicals	NB110-89474
Rat anti-mouse CD11b	1:200	Antibodies-online.com	ABIN474860
Goat anti-rat Cy3	1:200	Dianova	112–165-003
AF488-conjugated Isolectin-IB4	1:200	Invitrogen	I21411
FITC anti-mouse F4/80 clone BM8	1:100	Biolegend	123108
PerCP-Cy5.5 anti-mouse Ly6C clone HK1.4	1:200	Biolegend	128012
APC/Cy7 anti-mouse NK1.1 clone PK136	1:200	Biolegend	108724
PE anti-mouse CD45 clone 30-F11	1:200	BD Biosciences	553081
PE-Cy7 anti-mouse CD11b clone M1/70	1:200	BD Biosciences	561098
APC-Cy7 anti-mouse Ly6G clone 1A8	1:200	BD Biosciences	560600
AF405 anti-CD3 clone KT3	1:200	DRFZ Berlin, Germany	none

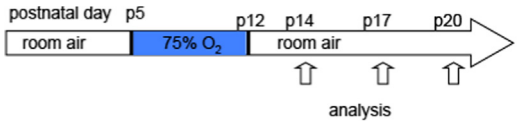

Fig. 1. Oxygen-induced retinopathy mouse model.

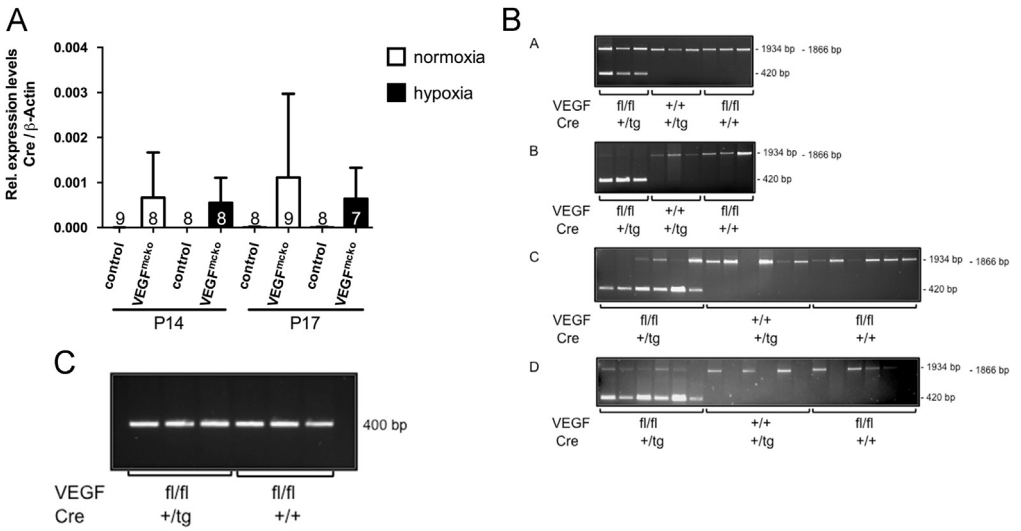

Fig. 2. Validation of the VEGF$^{fl/fl}$ LysMCre mouse model in the retina. (A) Relative Cre mRNA expression levels in the retina. Measurement of relative Cre mRNA expression levels by quantitative Real-Time PCR in VEGF^{mcko} and control mice under normoxic and hypoxic conditions (animal numbers per group are indicated in the figure on each bar) as an indirect indication of the occurrence of recombination in the retina on P14 (VEGF^{mcko} hypoxia $5.48\times10^{-4}\pm5.56\times10^{-4}$; VEGF^{mcko} normoxia $6.63\times10^{-4}\pm10.06\times10^{-4}$) and on P17 (VEGF^{mcko} hypoxia $6.46\times10^{-4}\pm6.85\times10^{-4}$; VEGF^{mcko} normoxia $11.13\times10^{-4}\pm18.58\times10^{-4}$). (Cre mRNA expression in the control tissues brain and bone marrow Fig. 3C, D). (B) Genomic recombination efficiency in various murine tissues. Detection of the length of the VEGF-A gene in thyme (A), brain (B), spleen (C) and bone marrow (D) in three mice per group of VEGF^{mcko} (VEGF$^{fl/fl}$ Cre$^{tg/+}$) and two types of control animals through genomic PCR analysis. DNA from the bone marrow and spleen was isolated after magnetic cell sorting of CD11b positive cells. A 420 bp fragment in VEGF^{mcko} mice (VEGF$^{fl/fl}$ Cre$^{tg/+}$) indicates the occurrence of recombination, a 1934 bp long fragment was found in the floxed and a 1866 bp long fragment in the wildtype control animals. (C) Screen for *Pdeb*^{rd1} mutation. Genomic PCR screen for a *Pdeb*^{rd1} mutation causing postnatal photoreceptor degeneration in three VEGF^{mcko} (VEGF$^{fl/fl}$ Cre$^{tg/+}$) and three control animals (VEGF$^{fl/fl}$ Cre$^{+/+}$). A 400 bp long fragment was proof of the presence of a wildtype allele and ruled out the presence of the mutation, which would have been indicated by a 550 bp long band.

All non-liposome treated mice were genotyped twice: on P12 ear punch tissue was used for DNA isolation. All animals were re-genotyped after completion of the experiment by tail tip biopsy. For the VEGF-A flox PCR the following primers were used: muVEGF419.F (5′-CCTGGCCCTCAAGTACACCTT-3′); muVEGF567.R (5′-TCCGTACGACGCATTTCTAG-3′). In the presence of a loxP-1 site these primers generated a 168 bp long fragment, and an approximately 100 bp long band in the wildtype. Evidence of the LysMCre transgene was shown using the following primers: IMR3066 (5′-CCCAGAAATGCCAGATTACG-3′); IMR3067 (5′-CTTGGGCTG CCAGAATTTCTC-3′); IMR3068 (5′-TTACAGTCGGCCAGGCTGAC-3′). Presence of the transgene was indicated by a 700 bp long band and the presence of a wildtype allele by a 350 bp long band.

3.2. Mouse organ dissection

Organs of mice were dissected for various reasons including genomic PCR, mRNA expression level analysis, histological analysis and flow cytometry. All mice were first narcotized using a mixture of 10 mg/g bodyweight ketamine (Ketamine-Actavis®, Actavice Group PTC ehf., Hafnarfjördur, Island)

and 0.015 mg/g bodyweight xylazine (CP-Pharma, Burgdorf, Germany) and then euthanized by cervical dislocation, and the tail tip was cut off for the second confirmation of the genotype. Both the femoral and the tibial bone were extracted from the leg, the bone marrow flushed out with a 20G syringe needle (B. Braun, Melsungen, Germany) into the tube with PBS, and centrifuged at 1400 rpm for five minutes. The thorax was cut open and thyme, spleen as well as the lungs were dissected and cleaned from blood as best as possible. The eyes were enucleated and dissected under microscopic control. Cornea and lens were removed and the retina carefully dissected out of the eyecup removing vitreous body and RPE cells as best as possible. Finally, the skull was cut open, the brain extracted and cut into halves.

A

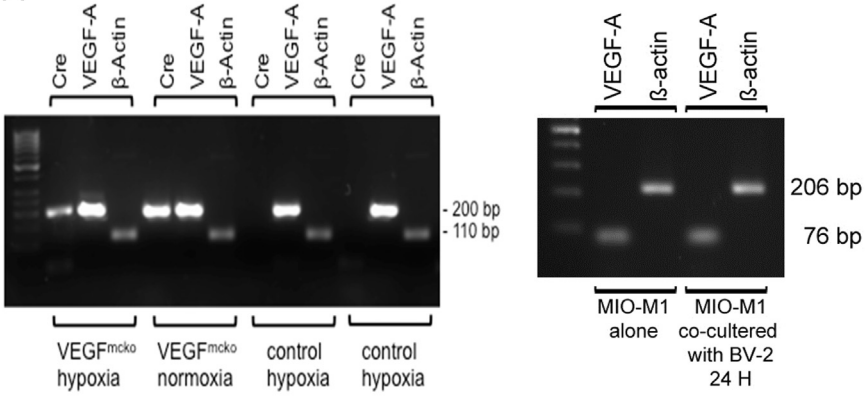

B

Beta-Actin

>14216676.seq - ID: D7-b-actin on 2014/8/29-2:33:43 automatically edited with PhredPhrap, start with base no.: 14 Internal Params: Windowsize: 20, Goodqual: 19, Badqual: 10, Minseqlength: 50, nbadelimit: 1

actTcacnCCCcaGCcnTGTACGTAGCcaTCCaGGCTGTGCTGTCCCTGT
ATGCCTCTGGTCGTACCACAGGCATTGTGATGGACTCCGGAGACGG
GGTCACCCACACTGTGCCCATCTACGAGGGCTATGcTCncccncacgccA
TCCTGCGTCTGGACCTGGCTGGCCGGgAcCTGACAGACTACCTCAT
GAagATCCTGAaccctaagGcCAACCGtga

VEGF-A

>14202452.seq - ID: B4-VEGF on 2014/8/28-12:23:16 automatically edited with PhredPhrap, start with base no.: 16 Internal Params: Windowsize: 20, Goodqual: 19, Badqual: 10, Minseqlength: 50, nbadelimit: 1

gangTtGCTCTCTGacGTGGGCACGCACTCcAGGGCTTCaTCGTTACaG
CAGCCTGCACAGCGCATCAGCGGCACACAGGACGGCTTGAAGATGT
ACTCTATCTCGTCGGGGTACTCCTGGAAGATGTCCACCAGGGTCTCA
ATCGGACGGCAATAG

Cre

>14202451.seq - ID: C1-Cre on 2014/8/28-12:23:15 automatically edited with PhredPhrap, start with base no.: 20 Internal Params: Windowsize: 20, Goodqual: 19, Badqual: 10, Minseqlength: 50, nbadelimit: 1

GnnAtACGTAATCTGGCATTTCTGGGGAtTGCTTATAACACCCTGTTAC
GTATAGCCGAAATTGCCAGGATCAGGGTTAAAGATATCTCACGTACTG
ACGGTGGGAGAATGTTAATCCATATTGGCAGAACGAAAACGCTGGtt

Fig. 3. Primer specificity analysis in the retina and cell culture Cre and VEGF-A mRNA expression analysis in relevant tissues and cells. (A) Left panel: Primer specificity in the retina was monitored by separation of the amplification product in the retina of $VEGF^{mcko}$ and control mice under normoxic und hypoxic conditions through a 2% agarose gel. The β-Actin primers amplified a 110 bp long product, the VEGF-A primers 201 bp product and the Cre primers a 195 bp long product. Right panel: Primer specificity in human MIO-M1 cells was monitored by separation of the amplification products through a 2% agarose gel. β-Actin primers amplified a 206 bp long product and the VEGF-A primers a 76 bp product. (B) After separation through an agarose gel, primer specificity was further verified by purification and subsequent sequencing of the amplification product. The graph shows the transcript sequence for the amplification product for each primer pair (β-Actin, VEGF-A, Cre). (C) Relative Cre mRNA expression levels in the brain. Measurement of relative Cre mRNA expression levels of $VEGF^{mcko}$ and control mice on P14 and P17 under normoxic and hypoxic conditions in the brain (animal numbers per group are indicated in the figure on each bar) (P14: control normoxia $2.18\times10^{-7} \pm 6.53\times10^{-7}$, $VEGF^{mcko}$ normoxia $7.76\times10^{-5} \pm 9.83\times10^{-5}$, control hypoxia 0 ± 0, $VEGF^{mcko}$ hypoxia 0 ± 0; P17: control normoxia $2.07\times10^{-6} \pm 1.07\times10^{-6}$, $VEGF^{mcko}$ normoxia 0.0038 ± 0.0078, control hypoxia $1.52\times10^{-6} \pm 2.91\times10^{-6}$, $VEGF^{mcko}$ hypoxia 0.00024 ± 0.00021). (D) Relative Cre mRNA expression levels in the bone marrow. Measurement of relative Cre mRNA expression levels of $VEGF^{mcko}$ and control mice on P14 and P17 under normoxic and hypoxic conditions in the bone marrow (animal numbers per group are indicated in the figure on each bar) (P14: control normoxia $7.89\times10^{-5} \pm 0.00017$, $VEGF^{mcko}$ normoxia 0.012 ± 0.0089, control hypoxia 0 ± 0, $VEGF^{mcko}$ hypoxia 0.01 ± 0.0028; P17: control normoxia $2.47\times10^{-6} \pm 3.95\times10^{-6}$, $VEGF^{mcko}$ normoxia 0.014 ± 0.0071, control hypoxia 0.00011 ± 0.00023, $VEGF^{mcko}$ hypoxia 0.007 ± 0.0016). (E) Relative VEGF-A mRNA expression levels in the brain (microglia cells). Measurement of relative VEGF-A mRNA expression levels of $VEGF^{mcko}$ and control mice on P14 and P17 under normoxic and hypoxic conditions in the brain (animal numbers per group are indicated in the figure on each bar) (P14 $VEGF^{mcko}$ normoxia 0.015 ± 0.015; P17 $VEGF^{mcko}$ normoxia 0.086 ± 0.049). (F) Relative VEGF-A mRNA expression levels in the bone marrow. Measurement of relative VEGF-A mRNA expression levels of $VEGF^{mcko}$ and control mice on P14 and P17 under normoxic and hypoxic conditions in the bone marrow (animal numbers per group are indicated in the figure on each bar) (P14: control normoxia 0.0093 ± 0.0037, $VEGF^{mcko}$ normoxia 0.0056 ± 0.0018, control hypoxia 0.013 ± 0.0046, $VEGF^{mcko}$ hypoxia 0.0082 ± 0.004; P17: control normoxia 0.0048 ± 0.0013, $VEGF^{mcko}$ normoxia 0.0046 ± 0.0007, control hypoxia 0.0083 ± 0.0069, $VEGF^{mcko}$ hypoxia 0.0034 ± 0.0006). (G) Relative VEGF-A mRNA expression levels in the lungs. Measurement of relative VEGF-A mRNA expression levels of $VEGF^{mcko}$ and control mice on P14 and P17 under normoxic and hypoxic conditions in the bone marrow (animal numbers per group are indicated in the figure on each bar). The lungs served as positive control organs for VEGF-A mRNA analysis. (P14 control normoxia 0.21 ± 0.072, $VEGF^{mcko}$ normoxia 0.183 ± 0.068,) control hypoxia 0.149 ± 0.031, $VEGF^{mcko}$ hypoxia 0.148 ± 0.017; P17 control normoxia 0.244 ± 0.031, $VEGF^{mcko}$ normoxia 0.221 ± 0.067, control hypoxia 0.23 ± 0.037).

3.3. DNA isolation for genotyping

For purification of total genomic DNA from different mouse tissues, the DNeasy Blood and Tissue Kit (Qiagen, Hilden, Germany) was used and the manufacturer's instructions were followed.

3.4. mRNA expression levels

For reverse transcription of cDNA, the “High-Capacity cDNA Reverse Transcription Kit” (Applied Biosystems, Darmstadt, Germany) was used and the manufacturer's instructions were followed. In this experimental setup, β-Actin was chosen as the housekeeping gene for control since oxygen treatment influences the expression levels of glyceraldehyde 3-phosphate dehydrogenase (GAPDH) in vitro [3]. Transcripts of interest were cDNAs encoding Cre and VEGF-A in the retina, bone marrow or brain. SensiFAST SYBR (BIOLINE, Luckenwalde, Germany) was used for quantitative Real-Time PCR purposes, and the manufacturer's instructions were followed. The following primers were used: VEGF-A fwd (5′-CAGCTATTG CCGTCCGATTGA GA-3′) and VEGF-A rev (5′-TGC TGG CTT TGG TGA GGT TTG AT-3′) amplifying a 201 bp long product; Cre fwd (5′-GATTTCGACCAGGTTCGTTC-3′) and Cre rev (5′-GCT AACCAGCGTTTTCGTTC-3′); β-Actin fwd (5′-AAGGCCAACCGTGAAAAGAT-3′) and β-Actin rev (5′-GTGGTACGACCAGAGGCATAC). The samples were analyzed in a LightCycler 480 and calculations were performed using the LightCycler software (Roche, Basel, Switzerland). All samples were run in triplicates and the melting curve of each product was monitored and probes with unspecific melting curves were excluded from the analysis. In order to verify the specificity of the primers that were

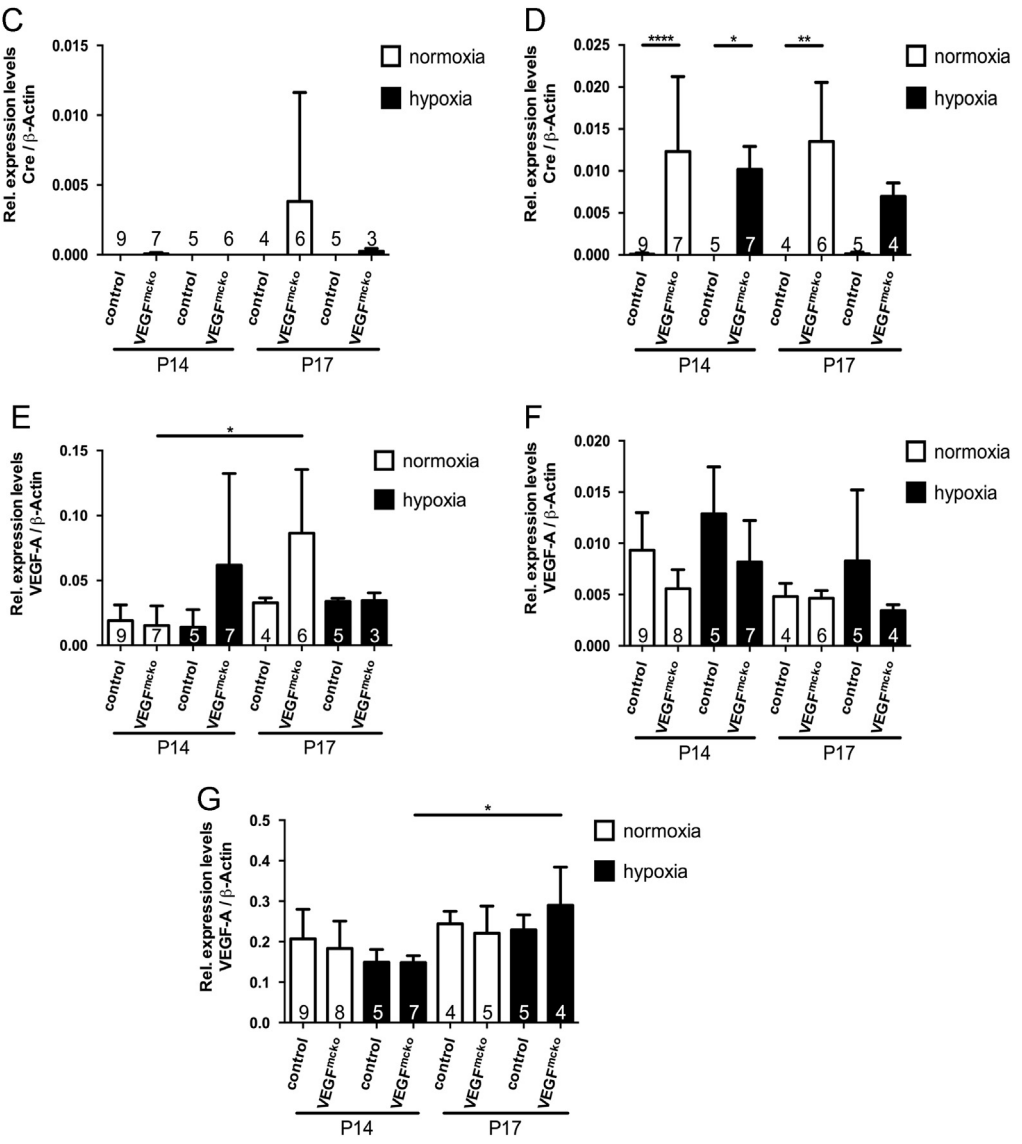

Fig. 3. (*continued*)

used, amplification products were separated on a 2% agarose gel, the DNA bands were purified from the agarose using QIAquick Gel Extraction Kit (Qiagen) and the manufacturer's instructions were followed before sequencing. Due to a very high amount of mRNA yield, the beta-Actin primers bound at a second binding site within the beta-Actin sequence, causing double peak melting curve. Sequencing of both peaks revealed that both products were beta-Actin products. Also the other products were primer specific.

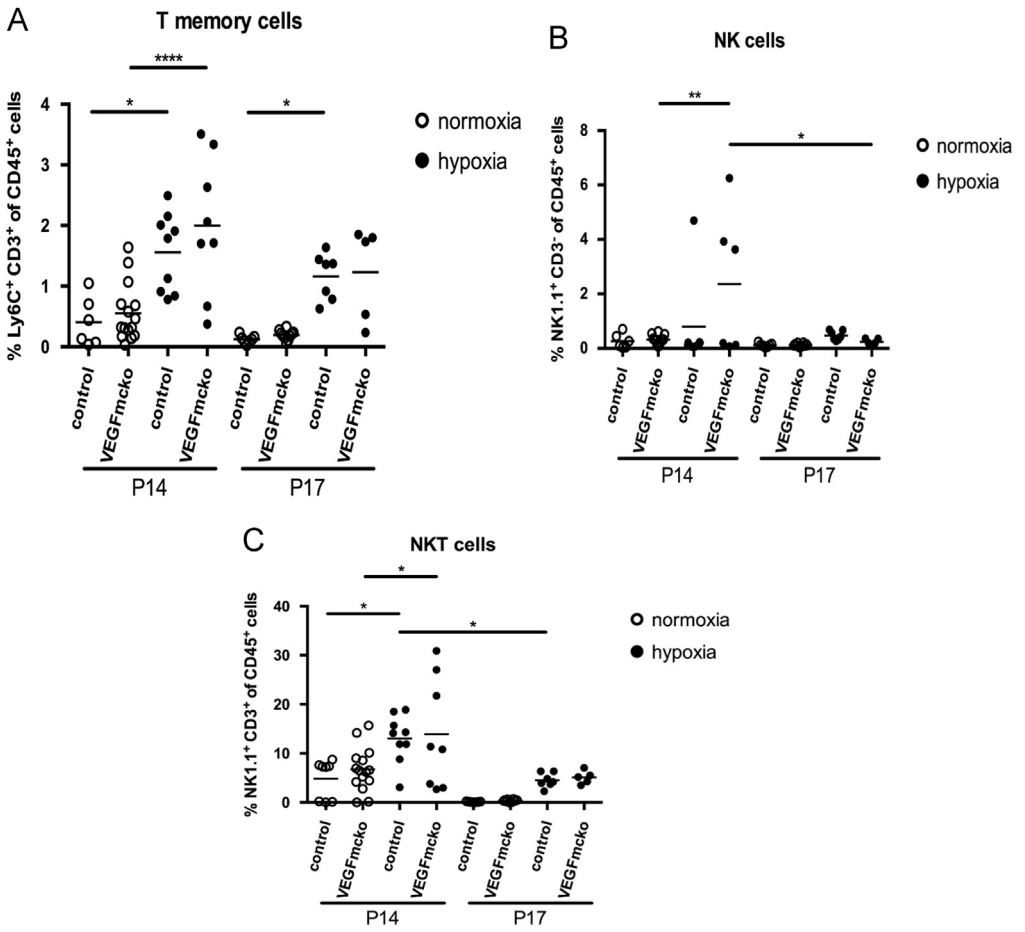

Fig. 4. Flow cytometry of T memory cells, natural killer (NK) cells, and natural killer-T (NKT) cells as percentage of CD45 positive cells in the retina. (A) T memory cells as percentage of CD45 positive cells (% $Ly6C^+CD3^+$ of $CD45^+$ cells): P14 hypoxia: $VEGF^{mcko}$ n=8; 2.0 ± 1.14%; control n=9; 1.56 ± 0.64%; P17 hypoxia: $VEGF^{mcko}$ n=5; 1.23 ± 0.78%; control n=7; 1.16 ± 0.38%. P14 normoxia: $VEGF^{mcko}$ n=15; 0.55 ± 0.48%; control n=6; 0.41 ± 0.41%; P17 normoxia: $VEGF^{mcko}$ n=10; 0.2 ± 0.08%; control n=7; 0.13 ± 0.07%. (B) NK cells as percentage of CD45 positive cells (% $NK1.1^+CD3^-$ of $CD45^+$ cells): P14 hypoxia: $VEGF^{mcko}$ n=6; 2.36 ± 2.61%; control n=7; 0.8 ± 1.71%. P14 normoxia $VEGF^{mcko}$ n=12; 0.32 ± 1.67%; control n=6; 0.26 ± 0.27%. P17 hypoxia $VEGF^{mcko}$ n=5; 0.24 ± 0.11%; control n=7; 0.47 ± 0.17%. P17 normoxia $VEGF^{mcko}$ n=10; 0.12 ± 0.05%; control n=7; 0.12 ± 0.07%. (C) NKT cells as percentage of CD45 positive cells (% $NK1.1^+CD3^+$ of $CD45^+$ cells): P14 hypoxia: $VEGF^{mcko}$ n=8; 13.91 ± 11.24%; control n=9; 13.02 ± 4.92%. P17 hypoxia: $VEGF^{mcko}$ n=5; 5.11 ± 1.35%; control n=7; 4.53 ± 1.47%. P14 normoxia: $VEGF^{mcko}$ n=15; 6.7 ± 4.43%; control n=8; 4.83 ± 3.93%. P17 normoxia: $VEGF^{mcko}$ n=10; 0.36 ± 0.23%; control n=7; 0.12 ± 0.07%.

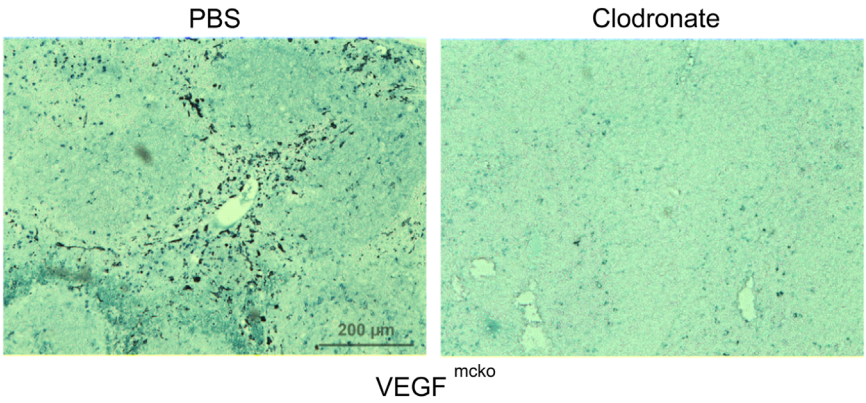

Fig. 5. Histochemistry of CD11b positive cells in spleen sections. Representative staining of CD11b positive cells in spleens of control mice kept under hypoxic conditions. Clodronate injection (right) led to a depletion of CD11b positive cells whereas sections of PBS injected controls (left) still showed a considerable amount of CD11b positive cells (dark staining).

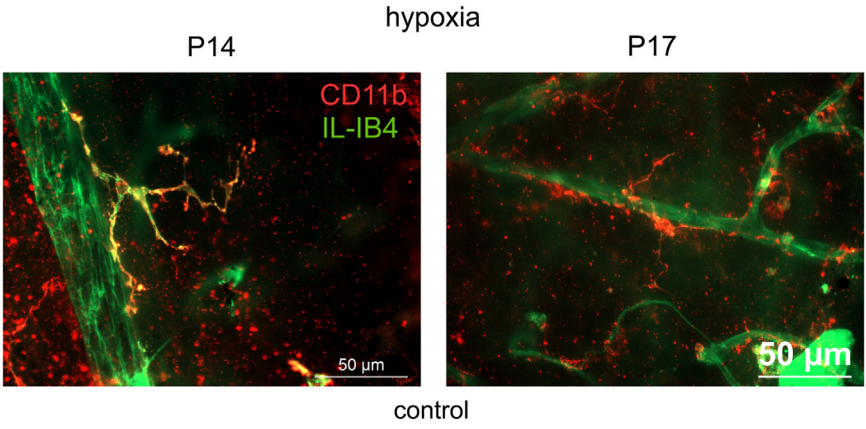

Fig. 6. Presence of mononuclear phagocytes (MPs) in close proximity to blood vessels. Representative images for mononuclear phagocytes (CD11b in red) and vessels (AF488-Isolectin-IB4 in green) of retinal flatmount preparations on P14 and P17 under hypoxic conditions in control mice.

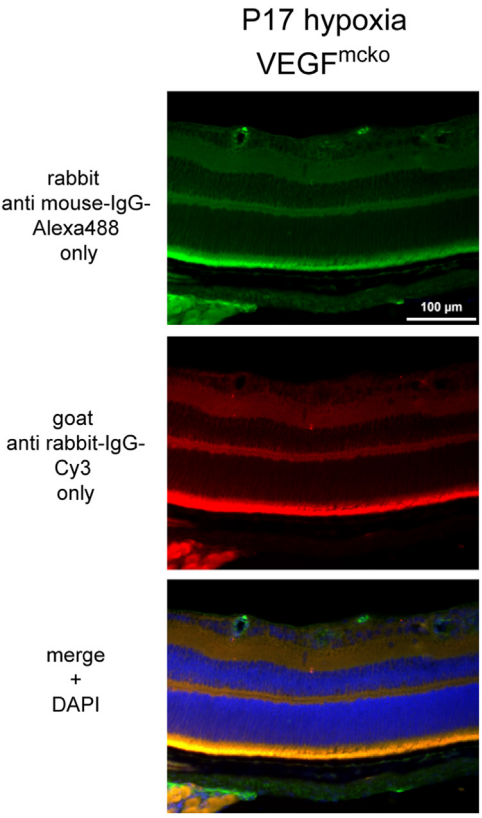

Fig. 7. Water control for vimentin and GFAP stainings for Müller cell activation. Representative images of water controls for vimentin (rabbit anti mouse-IgG-Alexa488 as secondary antibody) and GFAP (goat anti rabbit-IgG-Cy3 a secondary antibody) staining of Müller cells on P17 under hypoxic conditions in VEGF^{mcko} mice. The primary antibodies were omitted. Nuclei are co-stained with DAPI. Primary antibodies used: rabbit anti-GFAP (DAKO, Glostrup, Denmark) and monoclonal mouse anti-Vimentin antibody (Santa Cruz, Dallas, Texas, USA).

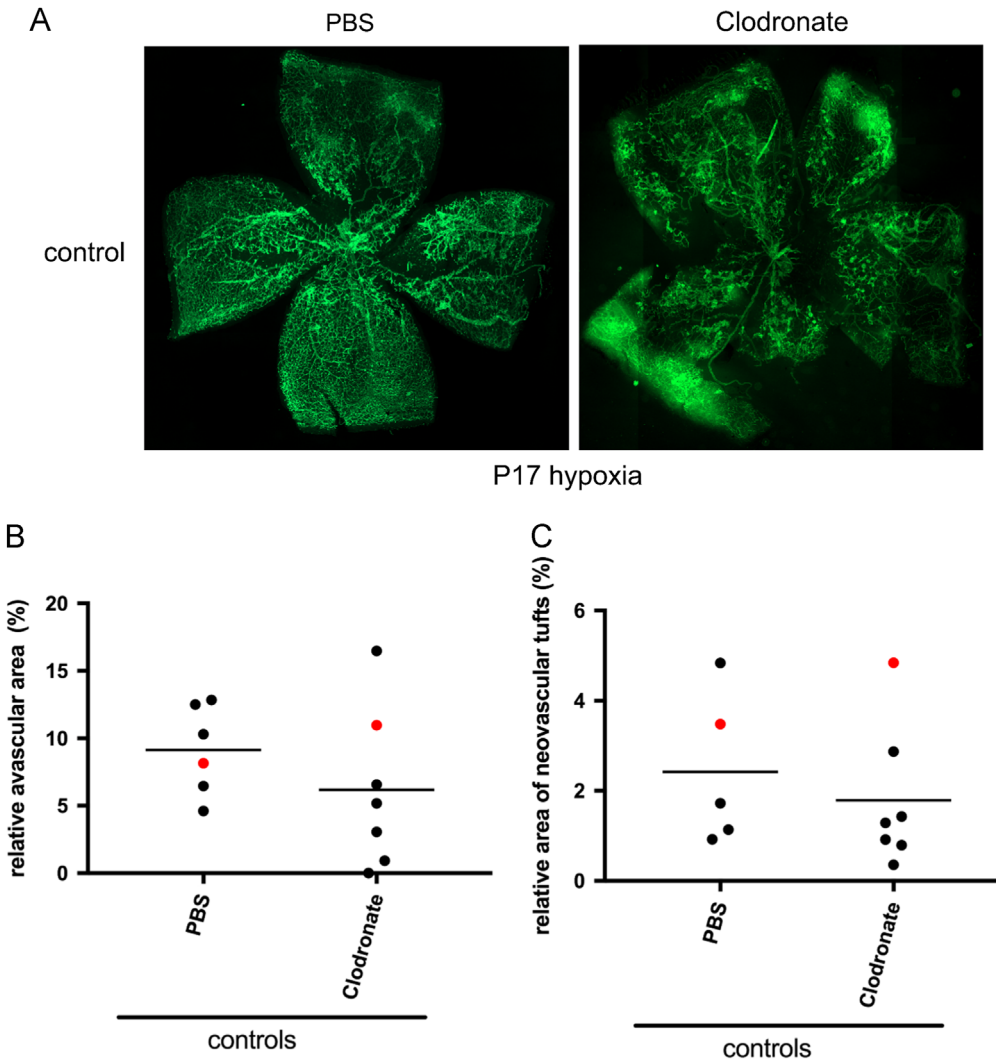

Fig. 8. Assessment of pathological retinal features in OIR in clodronate-liposome treated mice on P17. (A) Representative Isolectin IB4 staining of endothelial cells on retinal whole flatmounts. Images taken on P17 in control mice under hypoxic conditions in clodronate-liposome treated mice and the respective PBS-liposome treated controls. (B) Relative avascular area. Analysis of the avascular area relative to the total area of the whole flatmount on Isolectin-IB4 stained retinal flatmounts. Each symbol represents one individual mouse and red data points in every group indicate the matching images shown in (A). Clodronate n = 7, 6.17 ± 5.86%; PBS n = 6, 9.14 ± 3.32%. (C) Relative tuft area. Analysis of the tuft area relative to the total area of the whole flatmount on Isolectin-IB4 stained retinal flatmounts. Each symbol represents one individual mouse and red data points in every group indicate the matching images shown in (A). Clodronate n = 7, 1.79 ± 1.56%; PBS n = 5, 2.42 ± 1.68%.

Acknowledgments

We thank Dr. Napoleone Ferrara for kindly providing the VEGF-A flox line and Dr. Irmgard Förster for providing the LysMCre line. We thank Dr. Olaf Strauß for constructive discussion. Special thanks go to Dr. Fee Schmitt and Claudia Müller for her support in conducting the qPCR data, to Karin

Oberländer for embedding and cutting the paraffin sections, and to Gabriele Fels for support in conducting some immunostainings.

This study was funded by DFG Jo 324/10-2 (AMJ) and SFB 829 (SAE), a grant from the Christian and Emmy Sörensen Stiftung (CN), the Ilse-Palm Stiftung (AMJ), Bayer HealthCare AG, O_006_CHO (AMJ), a Marie Curie grant from the European Commission in the framework of the REVAMMAD ITN (Initial Training Research network), Project number 316990 (SC-G), and LOM of Charité Universitätsmedizin Berlin. Dr. Claudia Brockmann is participant in the BIH-Charité Clinical Scientist Program funded by the Charité - Universitätsmedizin Berlin and the Berlin Institute of Health.

Transparency document. Supporting information

Transparency data associated with this article can be found in the online version at https://doi.org/10.1016/j.dib.2017.11.062.

References

[1] C. Nürnberg, N. Kociok, C. Brockmann, T. Lischke, S. Crespo-Garcia, N. Reichhart, S. Wolf, R. Baumgrass, S.A. Eming, S. Beer-Hammer, A.M. Joussen, Myeloid cells contribute indirectly to VEGF expression upon hypoxia via activation of Müller cells Exp. Eye Res. 2017 in press.

[2] L.E. Smith, E. Wesolowski, A. McLellan, S.K. Kostyk, R. D'Amato, R. Sullivan, P.A. D'Amore, Oxygen-induced retinopathy in the mouse, Invest. Ophthalmol. Vis. Sci. 35 (1994) 101–111.

[3] H. Zhong, J.W. Simons, Direct comparison of GAPDH, beta-actin, cyclophilin, and 28S rRNA as internal standards for quantifying RNA levels under hypoxia, Biochem. Biophys. Res. Commun. 259 (1999) 523–526.